land

MDPI

Article

Urban–Rural Spatial Patterns, Landscape Configuration, and Carbon Emission Performance: A County-Level Analysis in Henan Province, China

Shaowei Zhang [1], Xiaoyang Guo [1], Shennian Zhang [2], Chen Li [1] and Chenming Zhang [1,*]

[1] School of Human Settlements, North China University of Water Resources and Electric Power, Zhengzhou 450046, China; zhangshaowei@ncwu.edu.cn (S.Z.); x20241141073@stu.ncwu.edu.cn (X.G.); x20241141054@stu.ncwu.edu.cn (C.L.)
[2] School of Architecture, Xi'an University of Architecture and Technology, Xi'an 710055, China; zsx132465798@xauat.edu.cn
* Correspondence: zhangchenming@ncwu.edu.cn

Abstract

Against the backdrop of global climate change and increasing pressure to mitigate carbon emissions, counties serve as critical units for urban–rural spatial development and carbon governance. However, their carbon emission performance (CEP) and underlying spatial mechanisms remain insufficiently understood. This study focuses on 157 counties in Henan Province, selecting three time points: 2013, 2018, and 2023. The study measures the CEP and analyzes its spatiotemporal differentiation characteristics. First, considering that carbon emissions are undesirable outputs generated during the economic production process, this study employs the undesirable output slack-based measure (UN_SBM) model and the super-efficiency slack-based measure model with undesirable outputs (Un_Super_SBM) to evaluate county-level carbon emission performance. Second, landscape pattern indicators, including expansion, complexity, and compactness, are selected, and regression models are constructed to explore the influence of different factors on carbon emission performance. The results show the following: (1) The overall CEP of counties in Henan Province improved from 2013 to 2023, but there were significant spatial differences. (2) Both "Total landscape area" (TA) and "Area-weighted mean shape index" (AWMSI) had significant positive impacts on CEP, whereas the "Splitting index" (SPLIT) inhibited CEP. (3) The effects of vegetation cover and transportation conditions varied, reflecting the heterogeneity of development stages and spatial functional positioning across different counties. This study reveals the relationship between urban–rural spatial form and carbon emission performance at the county level, providing empirical evidence for optimizing construction land spatial structure, enhancing CEP, and promoting regional low-carbon development.

Keywords: carbon emission performance; construction land; landscape patterns; county level; Henan province

Check for updates

Academic Editors: Le Yu and Jianjun Zhang

Received: 5 May 2026
Revised: 30 May 2026
Accepted: 8 June 2026
Published: 10 June 2026

Copyright: © 2026 by the authors. Licensee MDPI, Basel, Switzerland. This article is an open access article distributed under the terms and conditions of the Creative Commons Attribution (CC BY) license.

1. Introduction

Global climate change poses critical challenges to sustainable regional development, particularly in terms of reducing carbon emissions while improving environmental efficiency [1]. Among the indicators used to evaluate low-carbon development, carbon emission performance (CEP)—which measures the economic output achieved per unit of carbon emitted under specific input conditions—has emerged as a key indicator for

assessing the efficiency of economic development relative to carbon emissions [2–8]. Improving CEP is widely recognized as a crucial pathway to reconcile growth and emission reduction objectives [9].

Recent studies have increasingly emphasized that urban–rural spatial patterns and land-use morphology play important roles in shaping regional carbon emissions and carbon efficiency [10–12]. Existing research suggests that urban spatial configuration influences transportation demand, infrastructure utilization, land-use efficiency, and industrial agglomeration, thereby affecting carbon-related environmental performance [13–16]. Compact and contiguous urban forms are generally associated with lower commuting costs and more efficient infrastructure sharing, whereas dispersed and fragmented spatial patterns may increase energy consumption and reduce land-use efficiency [17,18].

At the landscape-pattern level, construction land metrics such as TA, AWMSI, and SPLIT have been widely used to characterize urban spatial morphology [19,20]. Previous studies indicate that larger and more concentrated construction land patches may improve carbon efficiency through economies of scale and centralized infrastructure systems [21]. In contrast, fragmented landscapes are often associated with higher transportation demand and spatial separation of urban functions, which may negatively affect carbon performance. However, existing findings remain inconsistent regarding the effects of landscape morphology and spatial configuration on carbon-related efficiency, suggesting that these relationships may vary across regions and development stages [22,23].

Existing research, however, exhibits several limitations. First, most studies focus on the provincial or city scale, overlooking counties, which are crucial units linking urban and rural development with heterogeneous land-use patterns [24–27]. Second, many studies analyze landscape patterns using aggregate land-use types without explicitly focusing on construction land, which is the primary carrier of carbon emissions. This may dilute the specificity of conclusions regarding the role of urban development in carbon efficiency [28–30]. Third, conventional cross-sectional multiple regression models often fail to capture spatial heterogeneity, limiting the identification of localized or mechanism-driven effects on CEP [13,31–34].

In China, counties represent the fundamental units of territorial governance, responsible for land-use planning, economic development, and the coordination of urban–rural systems. Compared with larger administrative units such as provinces or municipal-level regions, counties provide a finer spatial scale for capturing urban–rural heterogeneity and land-use differences. The substantial variation in economic development, industrial structure, and land-use intensity across counties also allows for detailed spatial analysis of carbon emission performance.

To address these gaps, this study focuses on 157 county-level administrative units in Henan Province, including both counties and county-level cities (hereafter collectively referred to as "counties"). Three time points (2013, 2018, and 2023) were selected to systematically measure CEP and analyze its spatiotemporal variation. The study is guided by three central research questions: (1) How do urban–rural spatial patterns, particularly construction land landscape characteristics, influence carbon emission performance at the county level? (2) Do these effects exhibit significant spatial heterogeneity across counties? (3) What mechanisms underlie the spatially varying impacts of landscape patterns on CEP? Answering these questions can provide insights for low-carbon spatial planning and targeted policy interventions at the county level.

To answer these questions, we employ an integrated analytical framework. County-level CEP is quantified using the UN_SBM model and Un_Super_SBM model [2–4]. Landscape metrics for construction land are constructed, including "Total landscape area" (TA), "Area-weighted mean shape index" (AWMSI), and "Splitting index" (SPLIT). Eco-

logical and infrastructure variables, such as "Mean Normalized Difference Vegetation Index" (NDVI_mean), "Road network density" (RoadD), and "Night-time light" (NTL) as a proxy for industrial activity and energy consumption, are incorporated as control variables [19,20,35]. Cross-sectional multiple regression is applied to identify global effects, while multiscale geographically weighted regression (MGWR) captures spatially varying local effects [31].

This approach provides a comprehensive assessment of both the overall and localized impacts of urban–rural spatial patterns on CEP. The study contributes to the literature and practice in three main ways: (1) It delivers a county-level assessment of CEP and its temporal dynamics, providing a finer spatial-scale perspective compared with broader provincial and municipal-level studies. (2) It clarifies how construction land landscape patterns affect carbon efficiency and the mechanisms through which spatial heterogeneity emerges, bridging land-use planning and low-carbon development research. (3) By revealing spatially heterogeneous mechanisms through MGWR, it provides actionable evidence for targeted policy interventions and low-carbon land-use planning at the county level.

The remainder of this paper is organized as follows: Section 2 introduces the study area, data sources, and methodology, including efficiency measurement and landscape pattern indicators. Section 3 presents the empirical results, including cross-sectional multiple regression and MGWR analyses. Section 4 discusses the spatial mechanisms and policy implications of urban–rural development patterns on CEP. Section 5 concludes with key findings and recommendations for low-carbon regional development.

2. Materials and Methods

2.1. Study Area

Henan Province is located in central China, along the middle and lower reaches of the Yellow River, spanning the Qinling–Huaihe transition zone. The terrain is mountainous in the west and south and flat in the east. As a populous province and major agricultural–industrial base, Henan has a high share of secondary industry and relies primarily on fossil fuels, creating pressure for carbon reduction [36,37]. The province comprises 157 county-level units, which serve as key spatial and governance units, exhibiting substantial variation in urban–rural development and spatial patterns [15,26]. Therefore, county-level analysis provides a representative perspective for examining the spatial mechanisms influencing carbon emission performance in the province [25,27].

Beyond the geographic and topographic characteristics shown in Figure 1, Henan Province also exhibits significant spatial heterogeneity in terms of urban development intensity, construction land configuration, and urban–rural landscape patterns. To provide a more intuitive understanding of these spatial characteristics, representative examples of different construction land configurations and corresponding ground-level landscapes are presented in Figure 2.

2.2. Study Data

CEP is calculated using the output indicators "CO_2 emissions" and "Gross Domestic Product" (GDP), along with the input indicators "Total population", "Electricity consumption", and "Industrial enterprise POI count". By incorporating these input–output indicators into the UN_SBM and UN_Super_SBM, the CEP can be derived. The carbon emission data are sourced from the Emissions Database for Global Atmospheric Research, with a precision of 1 km × 1 km. These data are processed using ArcGIS 10.8 to extract the total carbon emissions for Henan Province. Population data are sourced from the LandScan population dataset. The GDP and electricity consumption date are all obtained from www.gisrs.cn. The raw data for "urban landscape patterns" comes from open-source

Landsat TM data from the Remote Sensing and Digital Earth Research Institute of the Chinese Academy of Sciences for the years 2013, 2018, and 2023. The mask tool in ArcGIS is used to extract construction land, and the construction land is then imported into Fragstats 4.2 software to calculate urban landscape pattern indices. "Night-time lights" (NTL) data are sourced from https://dataverse.harvard.edu/dataset.xhtml?persistentId=doi:10.7910/DVN/GIYGJU (accessed on 2 May 2026). Other related data, including "NDVI" and "road network density", are sourced from www.gisrs.cn (see Table 1).

Table 1. The data source in this study.

Variable Type	Indicator	Description	Data Source
Dependent Variables (Y)	Input	Population	https://landscan.ornl.gov (accessed on 15 January 2026)
	Input	Electricity consumption	www.gisrs.cn
	Input	Industrial enterprise POI count	https://doi.org/10.5281/zenodo.15853565
	Desired output	GDP	www.gisrs.cn
	Undesired output	CO_2 emission	www.iea.org/data-and-statistics (accessed on 15 January 2026)
Independent Variables (X)	Landscape index metrics (X1~X3)	Total landscape area, TA (X1)	https://doi.org/10.5281/zenodo.15853565
		Area-weighted mean shape index, AWMSI (X2)	
		Splitting index, SPLIT (X3)	
	NDVI (X4)	NDVI_mean (X4)	www.gisrs.cn
	Road network density (X5)	RoadD (X5)	
	Night-time lights data (X6)	NTL (X6)	https://dataverse.harvard.edu/dataset.xhtml?persistentId=doi:10.7910/DVN/GIYGJU (accessed on 2 May 2026)

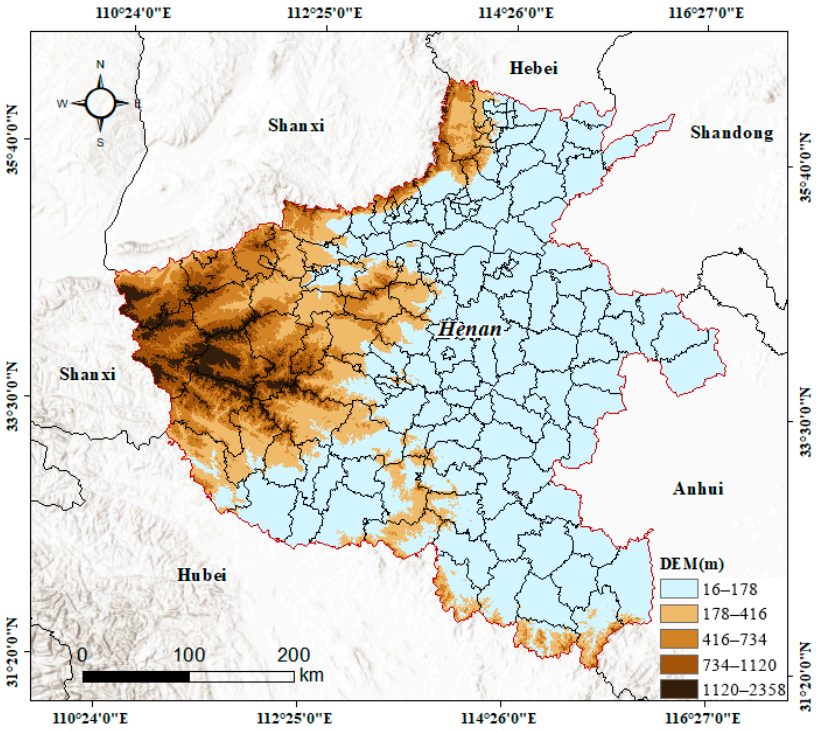


Figure 1. Location of the study area and county-level administrative units in Henan Province.

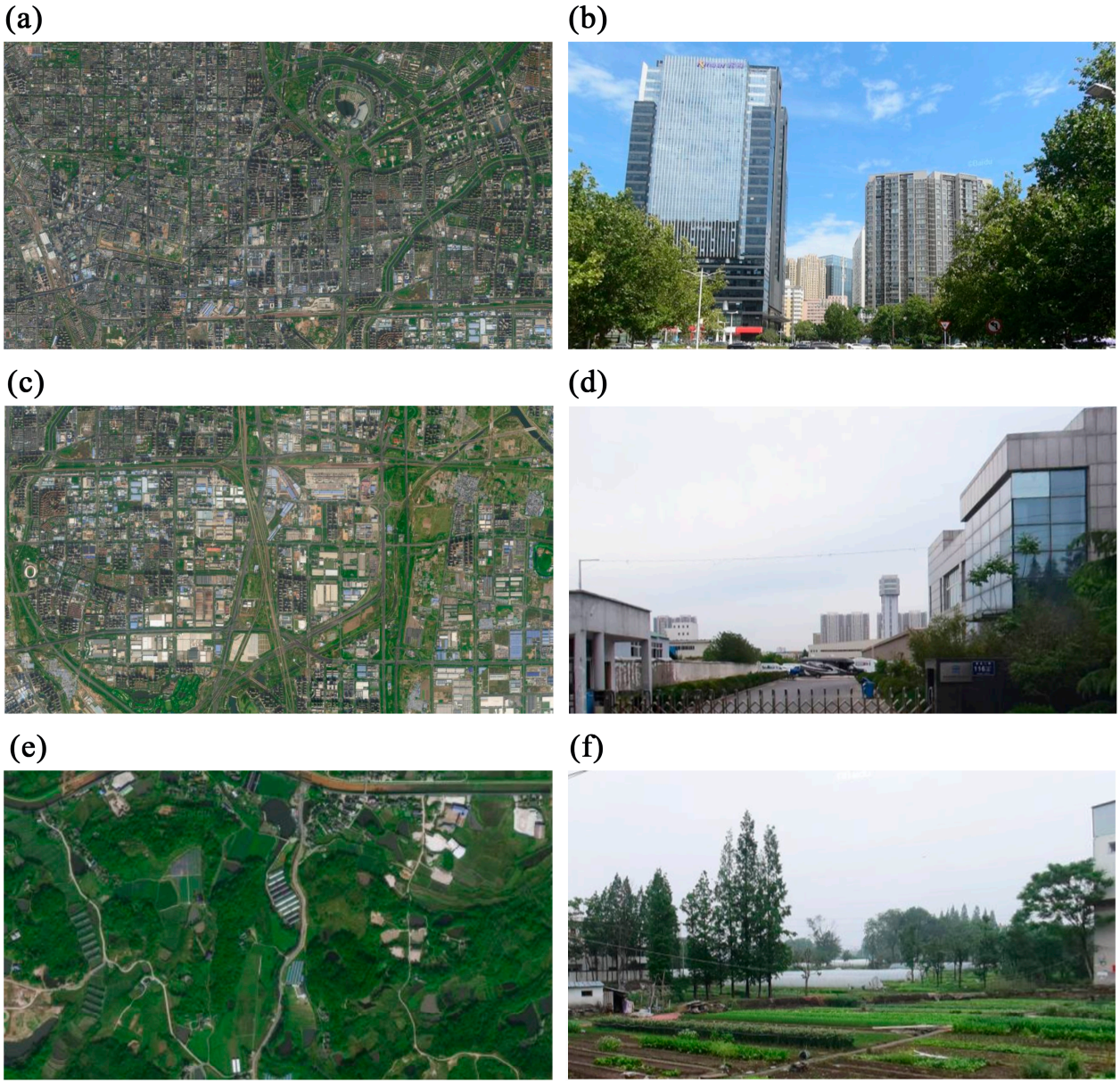


Figure 2. Representative construction land configurations and corresponding ground-level landscapes in Henan Province. Panels (**a**,**b**) show a compact construction land pattern associated with highly concentrated urban development and strong spatial continuity. Panels (**c**,**d**) illustrate a complex construction land morphology characterized by irregular patch boundaries and heterogeneous spatial configurations. Panels (**e**,**f**) depict a fragmented construction land pattern with dispersed settlements separated by agricultural and ecological spaces, reflecting a high degree of landscape fragmentation.

2.3. Methods

2.3.1. Research Framework

To systematically identify the influence mechanism of urban–rural spatial development patterns on CEP, this study constructs a three-stage research framework consisting of data collection and processing, methodological evaluation, and mechanism analysis (see Figure 3). By integrating multi-source spatial data, efficiency measurement models, and spatial econometric approaches, the framework aims to reveal the impacts of urban–rural spatial patterns on CEP from both global effects and spatial heterogeneity perspectives [6,13].

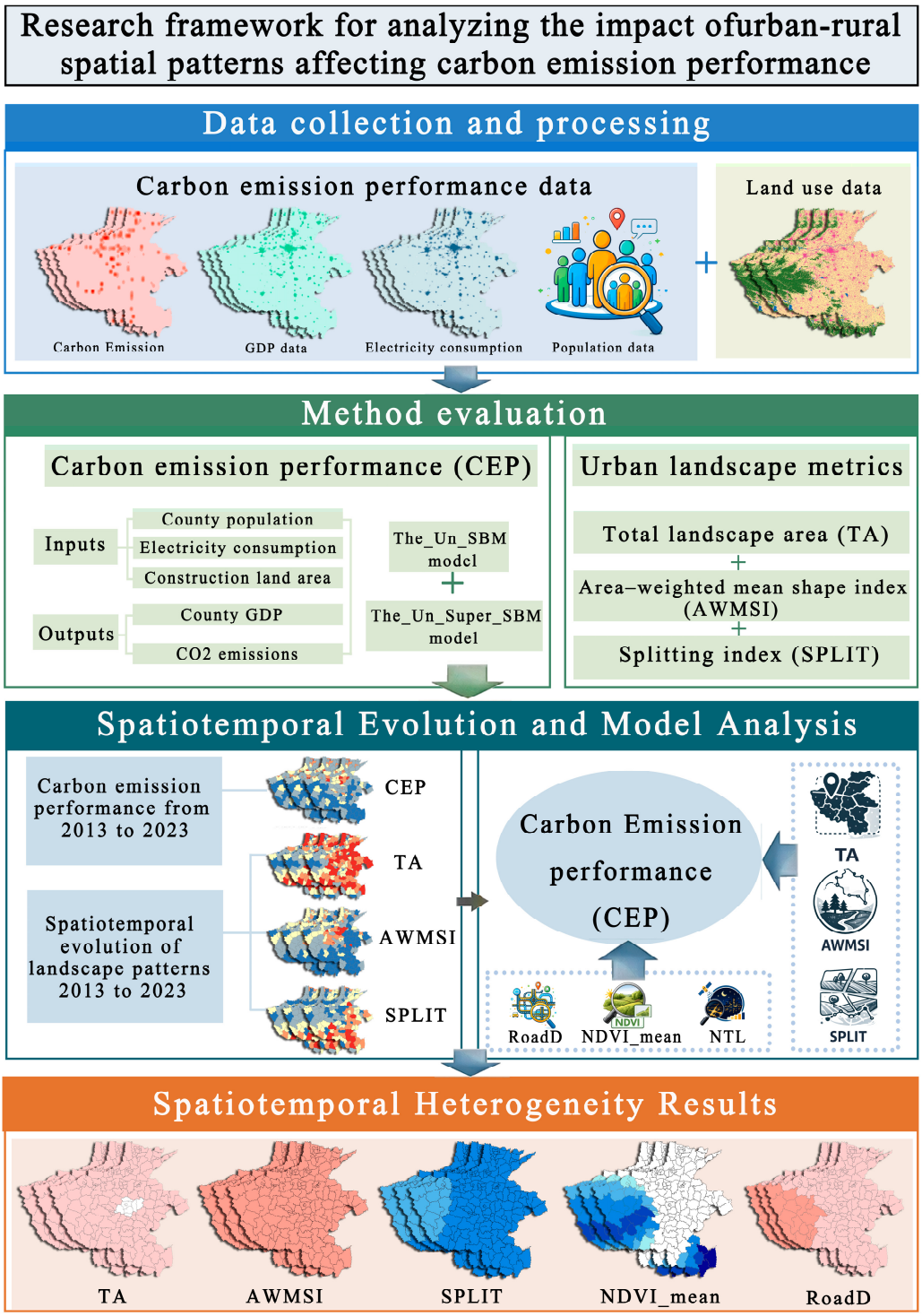


Figure 3. Analytical framework of the study.

First, during the data collection and processing stage, a comprehensive county-level dataset was established. The dataset primarily includes urban land-use data, carbon emission data, industrial enterprise POI data, and socioeconomic and ecological environment indicators. Land-use data were used to extract the spatial pattern characteristics of construction land; carbon emission data were employed to estimate county-level CO_2 emissions; and socioeconomic indicators, such as population, GDP, electricity consumption, together with industrial enterprise POI data, were all incorporated into CEP. The NDVI, RoadD, and NTL were used to represent ecological conditions, transportation infrastructure, and indus-

trial structure and energy consumption. All datasets correspond to three time points—2013, 2018, and 2023—and were processed and aligned through GIS-based spatial analysis.

Second, in the methodological evaluation stage, both carbon emission performance measurement and landscape pattern indicator construction are conducted. For the measurement of carbon emission performance, this study adopts the SBM model, which has been widely applied in efficiency evaluation under environmental constraints [4,9,38]. Additionally, the super-efficiency slack-based measure model with undesirable output model is employed to further distinguish efficiency frontier units, thereby obtaining CEP values for each county. In terms of landscape pattern indicators, construction land is taken as the research object, and three landscape metrics—TA, AWMSI, and SPLIT—are calculated to characterize urban–rural spatial development patterns from the dimensions of scale, morphology, and spatial structure [11,20].

Finally, in the mechanism analysis stage, regression models are constructed to identify the influence mechanisms of urban–rural spatial development patterns on CEP after obtaining CEP values and landscape pattern indicators. A cross-sectional multiple regression model is first applied to analyze the overall impacts of landscape pattern variables on CEP, with NDVI_mean, road network density, and NTL included as control variables. Considering that the relationships between variables may exhibit spatial non-stationarity, a spatial autocorrelation test is first conducted to assess the clustering patterns of carbon emission performance across counties, providing a basis for subsequent local regression analysis. Thereafter, MGWR model is introduced to capture the local effects and spatial heterogeneity of explanatory variables across different regions [31].

Overall, the proposed framework follows a progressive analytical pathway of "efficiency measurement–global regression–local spatial analysis", enabling a comprehensive understanding of both the overall mechanisms and spatially heterogeneous effects of urban–rural spatial development patterns on carbon emission performance. This framework provides a methodological basis for the subsequent empirical analysis.

2.3.2. Measurement of CEP

CEP evaluates the efficiency of economic activities in generating desirable outputs such as GDP while producing undesirable outputs such as CO_2 emissions. Since CO_2 emissions are undesirable outputs, traditional radial Data Envelopment Analysis (DEA) models cannot effectively handle slack variables. Therefore, this study adopts the Un_SBM model to evaluate county-level CEP. The Un_SBM model simultaneously accounts for input redundancy and output shortfall in the presence of undesirable outputs, thus avoiding potential biases caused by radial models.

Assume that there are no decision-making units (DMUs), with each county-level administrative unit in Henan Province treated as a DMU. Each DMU contains three types of variables: an input vector x ∈ Rm, a desirable output vector y ∈ Rs1, and an undesirable output vector z ∈ Rs2. Accordingly, the input matrix X, desirable output matrix Y, and undesirable output matrix Z are constructed. Under the assumption of constant returns to scale (CRS), the production possibility set P is defined as:

$$P = \{(x, y) \mid \lambda X \geq x, \lambda Y \geq y, \lambda Z \leq z, \lambda \geq 0 \quad (1)$$

where λ = [λ1, λ2, . . ., λn] T denotes the weight vector for reference DMUs.

For each DMU, the Un_SBM model minimizes the efficiency loss ρ as follows:

$$\rho = min \frac{1 - \frac{1}{m}\sum_{i=1}^{m} \frac{s_i^x}{x_{i0}}}{1 + \frac{1}{s_1 + s_2}\left(\sum_{k=1}^{s_1} \frac{s_k^y}{y_{k0}} + \sum_{l=1}^{s_2} \frac{s_l^x}{z_{l0}}\right)} s.t. \begin{cases} x_{i0} = \sum_{j=1}^{n} \lambda_j x_j + s_j^x, \forall i \\ y_{k0} = \sum_{j=1}^{n} \lambda_j y_j - s_k^y, \forall k \\ z_{l0} = \sum_{j=1}^{n} \lambda_j z_j + s_l^z, \forall l \\ s_i^x \geq 0, s_k^y \geq 0, s_l^z \geq 0, \lambda_j \geq 0 \end{cases} \quad (2)$$

where s_j^-, s_j^+, s_j^b denote the slack of inputs, desirable outputs, and undesirable outputs, respectively. A value of ρ = 1 indicates a fully efficient DMU, while ρ < 1 indicates efficiency loss, which can be reduced by decreasing inputs, reducing undesirable outputs, or increasing desirable outputs.

To further distinguish efficient units on the frontier, this study employs the Un_Super_SBM model, which allows for efficiency values greater than 1. In the Un_Super_SBM model, the DMU under evaluation is excluded from the reference set, ensuring that multiple efficient DMUs can be ranked. The Un_Super_SBM optimization problem is formulated as:

$$\rho = min \frac{1 + \frac{1}{m}\sum_{i=1}^{m} \frac{s_i^x}{x_{i0}}}{1 - \frac{1}{s_1 + s_2}\left(\sum_{k=1}^{s_1} \frac{s_k^y}{y_{k0}} + \sum_{l=1}^{s_2} \frac{s_l^x}{z_{l0}}\right)} s.t. \begin{cases} x_{i0} = \sum_{j=1}^{n} \lambda_j x_j + s_j^x, \forall i \\ y_{k0} = \sum_{j=1}^{n} \lambda_j y_j - s_k^y, \forall k \\ z_{l0} = \sum_{j=1}^{n} \lambda_j z_j + s_l^z, \forall l \\ s_i^x \geq 0, s_k^y \geq 0, s_l^z \geq 0, \lambda_j \geq 0 \end{cases} \quad (3)$$

In the empirical analysis, population size, industrial enterprise POI count, and total electricity consumption are selected as input indicators. GDP is used as the desirable output indicator, while CO_2 emissions are treated as the undesirable output indicator. Based on these variables, the carbon emission performance of 157 county-level administrative units in Henan Province is calculated for the years 2013, 2018, and 2023.

The CEP values obtained from the above method are subsequently used as the dependent variable in the econometric models to examine the influence of urban–rural spatial development patterns on carbon emission performance.

2.3.3. Measurement of Landscape Metrics

To quantify the spatial characteristics of construction land at the county level, three key landscape metrics were selected: TA, AWMSI, and SPLIT. These indicators were chosen because they together capture the essential dimensions of urban–rural spatial patterns—scale, shape complexity, and fragmentation—to capture complementary dimensions of urban spatial morphology. TA measures the overall size of construction land, reflecting urban expansion and development intensity. AWMSI quantifies the shape irregularity of patches, indicating morphological complexity, while SPLIT captures the degree of spatial fragmentation. By combining these three metrics, the model provides a comprehensive and sufficient representation of construction land patterns, ensuring that scale, morphology, and spatial configuration are all considered for analyzing their effects on carbon emission performance [11,19–21,39].

2.3.4. NDVI_Mean and Road Network Density Calculation

This study further considers the effects of vegetation coverage and transportation infrastructure on carbon emission performance. NDVI_mean is used to represent vegetation coverage within each county. NDVI_mean values range from −1 to 1, where higher positive values indicate greater vegetation abundance. Based on Landsat satellite imagery, NDVI_mean values are calculated and averaged within each county boundary to obtain NDVI_mean. This indicator reflects the level of vegetation coverage within each county and is closely associated with ecological and urban development conditions. Higher NDVI_mean values may influence CEP indirectly by affecting local energy consumption, urban heat environments, and land development intensity. For example, increased vegetation coverage can help reduce cooling-related energy demand through shading and temperature regulation effects, thereby lowering carbon emissions associated with energy consumption. At the same time, counties with high vegetation coverage are often characterized by lower construction intensity and industrial activity, which may also influence the balance between economic output and carbon emissions within the SBM efficiency framework. Therefore, NDVI_mean is incorporated as a control variable to capture the potential effects of ecological background conditions on county-level carbon emission performance [21,27,30,35].

In addition, RoadD is used to characterize the intensity of transportation infrastructure [40]. Road networks not only represent major sources of energy consumption and carbon emissions but also influence land-use patterns and travel efficiency. Higher road network density generally indicates more developed transportation systems and greater urbanization levels, which may increase traffic-related energy consumption. However, improved road connectivity may also optimize travel routes and enhance transportation efficiency. Therefore, road network density may exert both positive and negative effects on carbon emission performance. Including this indicator helps control for differences in transportation infrastructure across counties when analyzing the determinants of CEP [15,18,41,42].

2.3.5. Empirical Model Setting on the Driving Mechanism

After obtaining the CEP evaluation results and the indicators of influencing factors, regression models are constructed to quantitatively analyze the effects of landscape pattern characteristics and control variables on CEP. Considering that the study includes three time points (2013, 2018, and 2023), separate multiple regression models are estimated for each year to analyze the effects of landscape pattern characteristics and control variables on CEP. This repeated cross-sectional approach allows us to capture the inter-annual variation while controlling for county-level heterogeneity, providing a clearer understanding of the determinants of CEP across years.

In this study, the dependent variable is CEP, while the explanatory variables include the three landscape pattern indices (TA, AWMSI, and SPLIT), as well as NDVI_mean, RoadD, and NTL. The regression model can be expressed as follows:

$$\ln(CEP_{it}) = \alpha + \beta_1 TA_{it} + \beta_2 AWMSI_{it} + \beta_3 SPLIT_{it} + \beta_4 NDVI_mean_{it} + \beta_5 RoadD_{it} + \beta_6 NTL_{it} + \varepsilon_{it} \quad (4)$$

where $CEP_{i,t}$ is the dependent variable representing carbon emission performance. TA denotes the total area of urban construction land, AWMSI measures the shape complexity of construction land patches, and SPLIT reflects the fragmentation or spatial configuration of urban land. These three indicators serve as the core explanatory variables. Control variables include vegetation coverage $NDVI_mean_{i,t}$, $RoadD_{i,t}$, and night-time lights $NTL_{i,t}$. NDVI_mean reflects ecological conditions, RoadD is the ratio of road area to urban admin-

istrative area, and NTL serves as a proxy for industrial structure and energy consumption. The indices i and t denote county and year, respectively, and $\varepsilon_{i,t}$ is the random error term.

However, the conventional cross-sectional multiple regression model assumes that regression coefficients remain constant across space, which makes it difficult to capture the potential spatial heterogeneity among different counties. Considering that the effects of urban–rural spatial patterns on carbon emission performance may vary across counties, this study further applies the MGWR model to capture spatially heterogeneous local effects for each year [31].

Prior to applying MGWR, a global spatial autocorrelation test (Moran's I) was conducted for county-level CEP to verify the presence of spatial dependence. The results confirm significant positive spatial autocorrelation, providing empirical justification for using spatially explicit regression models.

The MGWR model allows explanatory variables to operate at different spatial scales. Its basic form can be expressed as:

$$\ln(CEP_i) = \beta_0(u_i, v_i) + \sum_{k=1}^{5} \beta_k(u_i, v_i) X_{ki} + \varepsilon_i \quad (5)$$

where (ui, vi) represents the geographical coordinates of county i, and βk(ui, vi) denotes the local regression coefficient of the k-th explanatory variable at spatial location i. Compared with the traditional geographically weighted regression (GWR) model, MGWR allows different explanatory variables to have different bandwidths, thereby more accurately capturing variations in the spatial scales at which different factors influence carbon emission performance.

In this study, an adaptive bisquare kernel function is adopted to construct the spatial weight matrix, and the optimal bandwidth is determined using the corrected Akaike information criterion (AICc). The MGWR estimation results provide local regression coefficients and their significance levels for each variable across different counties, which are used to analyze the spatial heterogeneity of the impacts of urban–rural spatial development patterns on carbon emission performance.

By combining cross-sectional multiple regression model with the MGWR model, this study not only identifies the overall effects of influencing factors on carbon emission performance but also reveals their spatially varying relationships across regions, thereby providing a basis for subsequent spatial differentiation analysis.

3. Results

3.1. Spatiotemporal Patterns of CEP in Henan Province

As shown in Table 2, the mean CEP of county-level units in Henan Province increased from 0.319 in 2013 to 0.335 in 2023, indicating a modest overall improvement in carbon emission performance. Meanwhile, the standard deviation remained relatively high, suggesting persistent spatial heterogeneity across counties. The spatial distribution of CEP is further illustrated in Figure 4.

Table 2. Descriptive statistics and county distribution of CEP in Henan Province. Panel (**A**): descriptive statistics of CEP. Panel (**B**): county distribution across CEP categories.

(**A**)				
Year	Mean	SD	Min	Max
2013	0.319	0.204	0.080	1.343
2018	0.322	0.193	0.133	1.442
2023	0.335	0.221	0.128	1.559

Table 2. *Cont.*

(**B**)			
CEP Category	2013	2018	2023
Low	38	33	40
Medium–low	73	79	65
Medium	25	28	33
Medium–high	11	9	8
High	10	8	11
Total	157	157	157

CEP categories were classified as low (0.08–0.20), medium–low (0.20–0.35), medium (0.35–0.45), medium–high (0.45–0.65), and high (>0.65).

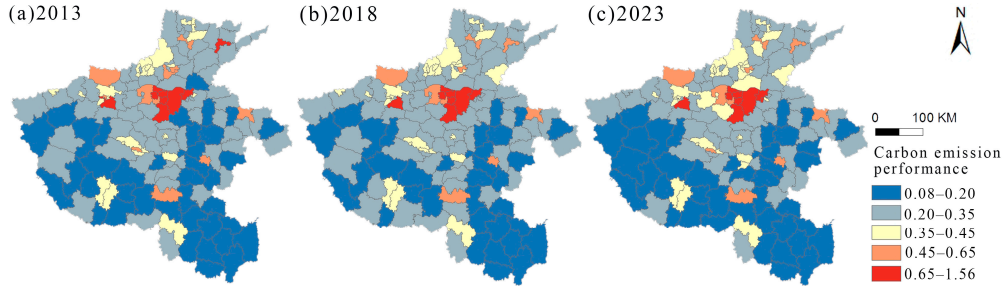


Figure 4. Spatial distribution of carbon emission performance in 2013, 2018, and 2023.

In 2013, county-level CEP in Henan Province exhibited pronounced spatial heterogeneity. Counties with high CEP values were mainly located in the northeastern and parts of the central-eastern regions, while counties with medium CEP values were distributed in the central and some eastern areas. Low-CEP counties were primarily found in the southwestern and southern regions. Statistical analysis indicates that high-CEP counties displayed significant spatial clustering, suggesting that these areas had achieved preliminary success in carbon management and industrial structure optimization. Many of these high-performance counties are located in regions with relatively advanced industrial development or ongoing low-carbon transition initiatives, which may partly contribute to their higher CEP levels through improved energy management and more efficient industrial organization.

By 2018, high-CEP counties had slightly expanded toward central regions, with northeastern counties remaining high performing. The coverage of medium-CEP counties further extended to parts of the central region, while low-CEP counties remained concentrated in the southwest and south. Notably, counties in the central-eastern region experienced relatively larger CEP increases, which may be partly associated with regional industrial upgrading and improvements in energy-use efficiency during the study period. For instance, some industrial clusters implemented the exit of high-energy-consuming industries and promoted the adoption of cleaner energy, thereby improving carbon emission efficiency per unit of GDP.

By 2023, high-CEP counties further stabilized in the northeastern and central-eastern regions, the coverage of medium-CEP counties continued to expand across central counties, and the number of low-CEP counties declined significantly. Statistical analysis demonstrates significant spatial heterogeneity of CEP at the county level. From a policy perspective, the observed improvements in CEP in some central and eastern counties may reflect broader trends of industrial upgrading and increasing attention to low-carbon development during recent years. Conversely, southwestern and southern counties, characterized by heavy industrial structures and a high proportion of energy-intensive enterprises, still exhibited low CEP, indicating differences in policy implementation and industrial transformation across regions. Overall, the spatial distribution of CEP is closely associated

with local economic development levels, industrial restructuring, energy consumption management, and policy execution, providing empirical support for formulating regionally differentiated carbon reduction policies.

Overall, the spatiotemporal evolution of county-level CEP in Henan Province during the study period can be characterized by overall improvement, stable spatial structure, and increasing regional disparities. Both high-value and low-value clusters exhibited relatively strong spatial stability, providing an empirical basis for further analysis of the impacts of landscape patterns and related factors on carbon emission performance.

3.2. Spatiotemporal Patterns of Urban Landscape Pattern in Henan Province

In 2013, counties with relatively high values of TA were mainly distributed in the central and some eastern parts of Henan Province, whereas counties in the western and southwestern regions were predominantly characterized by lower TA values. By 2018, the number of counties with high TA values increased significantly. The spatial distribution of these counties expanded from the central core region toward the eastern and southern parts of the province, and several counties that were previously at medium levels transitioned into high-value areas. Compared with 2018, the number of counties with high TA values further increased in 2023, forming a relatively continuous distribution pattern in the central region of the province. Overall, the scale of construction land exhibited a continuous expansion trend during the study period.

Counties with higher AWMSI values generally correspond to construction land patches with more complex shapes. In 2013, counties with high AWMSI values were mainly concentrated in the central region of the province, while counties in the western and southern areas exhibited relatively low values. By 2018, the number of counties with high AWMSI values increased and formed a more pronounced clustering pattern in the central region, while scattered high values also appeared in several counties in the eastern and northern parts of the province. By 2023, the spatial distribution pattern of high AWMSI counties remained relatively stable, still concentrated in the central core area, with only a few peripheral counties showing relatively low levels.

Higher SPLIT values indicate a higher degree of spatial fragmentation of construction land. In 2013, counties with high SPLIT values were mainly distributed in the southern and southeastern parts of Henan Province, whereas counties in the western and parts of the north-central regions exhibited relatively low values. In 2018, the spatial distribution of high-SPLIT counties showed some adjustments but remained largely concentrated in the southern region. By 2023, the number of counties with high SPLIT values decreased, and their spatial distribution gradually contracted. More counties exhibited medium or low levels, suggesting that the overall fragmentation of construction land in the province had somewhat alleviated. One possible explanation is that ongoing urbanization and infrastructure development have gradually increased the spatial connectivity of construction land, thereby reducing the degree of fragmentation. In addition, land consolidation and rural settlement reorganization policies implemented in some areas may have promoted the integration of scattered construction land patches. However, these potential mechanisms require further verification through policy and land-use transition analyses.

Overall, the landscape pattern of construction land across counties in Henan Province exhibited clear spatiotemporal dynamics during the study period. The scale of construction land continued to expand, counties with higher shape complexity remained largely concentrated in the central region, and the degree of construction land fragmentation showed a general shift from higher levels toward moderate or lower levels. The spatial distribution and evolutionary trends of different landscape pattern indicators varied con-

siderably, reflecting the diversity of county-level construction land in terms of expansion scale, morphological evolution, and spatial organization (see Figure 5).

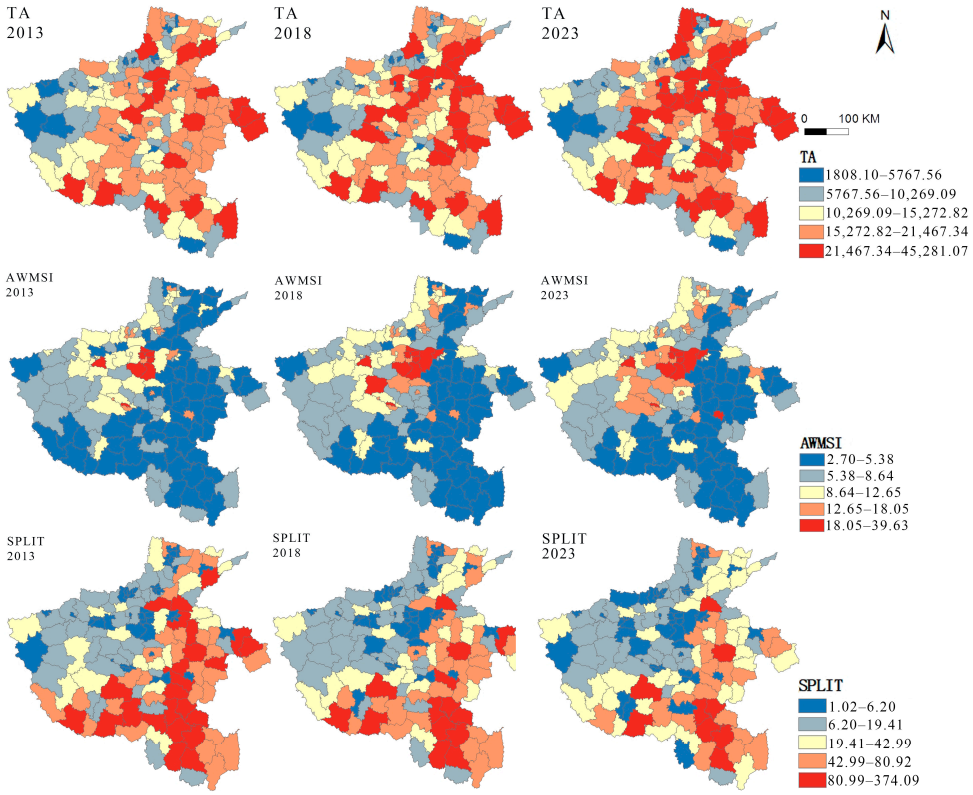


Figure 5. Spatial distribution of landscape pattern performance in 2013, 2018, and 2023.

3.3. Spatial Autocorrelation Analysis

Moran's I is a widely used measure of global spatial autocorrelation that quantifies the degree to which a variable exhibits spatial clustering across a study region. Specifically, it evaluates whether similar or dissimilar values of a variable are spatially clustered, dispersed, or randomly distributed. The index ranges from −1 to +1: a positive value indicates spatial clustering of similar values, a negative value indicates spatial dispersion or neighboring dissimilar values, and a value near zero suggests a random spatial pattern. Moran's I is commonly applied in geographic, environmental, and socioeconomic studies to assess the presence of spatial dependence, detect spatial patterns, and guide the selection of appropriate spatial econometric models. In the context of carbon emission performance analysis, Moran's I provides insight into whether high- or low-performance counties tend to cluster geographically, which is critical for understanding regional patterns and informing policy interventions.

To examine the spatial distribution characteristics of county-level CEP, a global Moran's I test was conducted for the years 2013, 2018, and 2023 (see Table 3).

Table 3. Global Moran's I test results.

Year	Moran's I	z-Score	*p*-Value
2013	0.4588	9.704	<0.001
2018	0.4912	10.475	<0.001
2023	0.5307	11.147	<0.001

Moran's I measures the degree of spatial autocorrelation, ranging from −1 (perfect dispersion) to +1 (perfect clustering). The z-score indicates how many standard deviations the observed Moran's I is from the expected value under spatial randomness. The *p*-value tests the statistical significance of the observed spatial pattern; $p < 0.05$ indicates significant spatial clustering.

As shown in Table 3, the Moran's I values for all three years are positive and statistically significant ($p < 0.001$), indicating that county-level CEP in Henan Province exhibits strong spatial dependence. High-CEP counties tend to be surrounded by other high-CEP counties, while low-CEP counties are near other low-CEP counties. Over time, the Moran's I values and corresponding z-scores increase, demonstrating that the spatial clustering of CEP becomes more pronounced and the high- and low-performance counties show stronger spatial aggregation.

These spatial autocorrelation results suggest that CEP exhibits significant non-random spatial patterns, providing a theoretical basis for applying the MGWR model. MGWR allows for the capture of local effects and spatial heterogeneity of explanatory variables on CEP across counties, thereby complementing the limitations of traditional global regression models in addressing spatial effects.

3.4. Multicollinearity Test

Prior to regression analysis, Pearson correlation analysis and variance inflation factor (VIF) tests were conducted to assess multicollinearity among explanatory variables. The results indicate that all VIF values are below the commonly accepted threshold of 10, suggesting that severe multicollinearity does not pose a significant problem in the models (see Table 4).

Table 4. Variance inflation factor (VIF) values of explanatory variables.

Variable	2013	2018	2023
β_1	1.459	1.545	1.704
β_2	2.658	2.321	2.280
β_3	1.729	2.019	2.341
β_4	3.314	3.848	3.926
β_5	3.078	5.546	3.813
β_6	3.911	4.145	3.225

β_1 = ln(TA), β_2 = AWMSI, β_3 = SPLIT, β_4 = NDVI_mean, β_5 = ln(RoadD), and β_6 = NTL. All VIF values are below the commonly accepted threshold of 10, indicating that severe multicollinearity is not present in the regression models.

3.5. Regression Results

3.5.1. Cross-Sectional Multiple Regression Results

Here, we present the regression results of the cross-sectional multiple regression models for 2013, 2018, and 2023. All core explanatory variables, including the landscape pattern metrics TA, AWMSI, and SPLIT, and control variables NDVI_mean and RoadD, show statistically significant effects on county-level carbon emission performance in 2013 and 2018. By 2023, NTL is no longer significant, while the remaining variables remain robust, indicating stable influences over time (see Table 5).

TA shows a consistently positive effect on county-level carbon emission performance across 2013, 2018, and 2023, with coefficients of 0.280, 0.202, and 0.165, respectively. All three years show statistically significant results, indicating that the expansion of construction land at the county level is associated with an increase in carbon emission performance. The magnitude of the effect slightly decreases over time, but TA remains an important positive contributor to CEP.

AWMSI shows a consistently positive and statistically significant effect on county-level carbon emission performance across the three years. The coefficients are 0.225 in 2013, 0.435 in 2018, and 0.333 in 2023, indicating that more complex and irregular urban patch shapes tend to enhance carbon emission performance. The positive effect is particularly strong in

2018, suggesting that during this period, shape complexity had the largest contribution to improving CEP, while it remains moderately strong in 2023.

Table 5. Coefficient (T-value).

Variable	2013 Coefficient (T-Value)	2018 Coefficient (T-Value)	2023 Coefficient (T-Value)
β_1	0.280 (5.125 ***)	0.202 (4.348 ***)	0.165 (3.458 ***)
β_2	0.225 (3.085 ***)	0.435 (7.634 ***)	0.333 (6.040 ***)
β_3	−0.262 (−4.469 ***)	−0.216 (−4.069 ***)	−0.245 (−4.387 ***)
β_4	−0.274 (−3.373 ***)	−0.154 (−2.094 **)	−0.139 (−1.918 *)
β_5	0.114 (1.456)	0.204 (2.311 **)	0.341 (4.783 ***)
β_6	0.256 (2.895 ***)	0.132 (1.728 *)	0.096 (1.456)
F	58.606	93.946	99.722

Dependent variable: ln(CEP). *, **, and *** indicate significance at the 10%, 5%, and 1% levels, respectively. β_1 = ln(TA), β_2 = AWMSI, β_3 = SPLIT, β_4 = NDVI_mean, β_5 = ln(RoadD), and β_6 = NTL.

SPLIT consistently exhibits a negative impact on county-level carbon emission performance across all three years. The coefficients are −0.262 in 2013, −0.216 in 2018, and −0.245 in 2023, all statistically significant. This indicates that higher landscape fragmentation, reflected by larger SPLIT values, tends to inhibit carbon emission performance. In other words, counties with more dispersed and fragmented construction land patches generally show lower carbon efficiency, highlighting the adverse effect of spatial disaggregation on CEP.

NDVI_mean shows a consistently negative effect on county-level carbon emission performance across the three years, with coefficients of −0.274 in 2013, −0.154 in 2018, and −0.139 in 2023. The variable is statistically significant in all years except 2023 at the 10% level, indicating that higher vegetation coverage within counties tends to slightly reduce measured CEP. This may reflect that areas with more natural vegetation have lower industrial activity or construction intensity, which affects the relationship between land use and carbon efficiency.

RoadD exhibits a positive effect on county-level carbon emission performance, with coefficients of 0.114 in 2013, 0.204 in 2018, and 0.341 in 2023. It is statistically significant only in 2018 and 2023, suggesting that higher road network density may contribute to better carbon efficiency in some years, potentially by facilitating more efficient transportation and energy distribution. However, the 2013 result is not significant, indicating that the impact of road infrastructure on CEP may vary over time and across counties.

NTL positively affects county-level CEP in 2013 and 2018, with coefficients of 0.196 and 0.145, both significant. By 2023, the effect weakens and becomes insignificant, suggesting that regions with higher industrial activity initially exhibit higher CEP, but this influence diminishes over time, likely due to improved energy efficiency or industrial restructuring.

Overall, the cross-sectional multiple regression results show substantial stability across the three study years. The directions of influence for the core explanatory variables, including TA, AWMSI, and SPLIT, remain consistent, while the control variables NDVI_mean, RoadD, and NTL generally retain their expected effects. Most variables are statistically significant across the years; however, NTL is no longer significant in 2023. These results suggest that the impact mechanism of urban–rural spatial development patterns on county-

level carbon emission performance is largely persistent over time, providing a reliable foundation for subsequent spatial heterogeneity analysis using geographically weighted regression models [14,17].

3.5.2. MGWR Results

The MGWR results reveal substantial spatial heterogeneity in the effects of county-level landscape and ecological variables on CEP across Henan Province for 2013, 2018, and 2023. NTL was also included as a control, but its effect remained relatively stable across counties and years, showing limited spatial variation (see Table 6 and Figure 6).

Table 6. MGWR regression coefficients of explanatory variables.

Variable	2013	2018	2023
β_1	0.411 (109)	0.223 (157)	0.120 (148)
β_2	0.438 (49)	0.468 (157)	0.326 (157)
β_3	−0.336 (157)	−0.175 (157)	−0.239 (157)
β_4	−0.305 (157)	−0.162 (121)	−0.240 (18)
β_5	0.267 (29)	0.212 (157)	0.382 (157)

Dependent variable: ln(CEP). β_1 = ln(TA), β_2 = AWMSI, β_3 = SPLIT, β_4 = NDVI_mean, and β_5 = ln(RoadD). Values in parentheses denote the number of samples significant at the 5% level.

For TA, the positive influence on CEP is most pronounced in the northeastern and central-eastern counties, particularly in 2013, while the effect weakens and becomes more uniform across the province in 2018 and 2023. This indicates that the scale of construction land has a locally variable effect on carbon efficiency, with the strongest benefits concentrated in counties with relatively intensive urban development. Counties with larger construction land in these regions often coincide with more advanced infrastructure, better access to energy-saving technologies, and more intensive industrial oversight, facilitating higher carbon efficiency.

AWMSI, representing shape complexity, shows a clear positive spatial effect, with higher values in central and eastern counties, especially in 2018 and 2023. Counties in the west and southwest exhibit lower or non-significant effects. This suggests that more irregular and complex urban land shapes, often resulting from compact and well-planned urban expansions, contribute to improved CEP by enabling efficient land utilization and spatially concentrated industrial activity.

The SPLIT index consistently exerts a negative effect on CEP, reflecting that landscape fragmentation inhibits carbon emission performance. This negative effect is strongest in central and southern counties in 2013, while by 2018 and 2023 it becomes more evenly distributed, suggesting that urban planning policies and land-use regulations gradually mitigate the detrimental impact of fragmented landscapes. Fragmented land may increase energy demand for transport and reduce the efficiency of industrial clustering, while more aggregated urban forms facilitate coordinated low-carbon interventions.

NDVI_mean shows negative effects in most counties in 2013, particularly in the south and west, suggesting that areas with denser vegetation tend to have lower CEP, likely due to lower industrial intensity or urbanization. By 2018 and 2023, this effect diminishes in central counties, reflecting a moderation of ecological influence as industrial and urban development patterns evolve. Road density positively affects CEP, especially in southern and central-eastern counties in 2023, highlighting the role of transportation connectivity in facilitating efficient logistics, centralized energy use, and better industrial distribution. Effects are weaker in northern counties due to differences in local economic structure and infrastructure capacity.

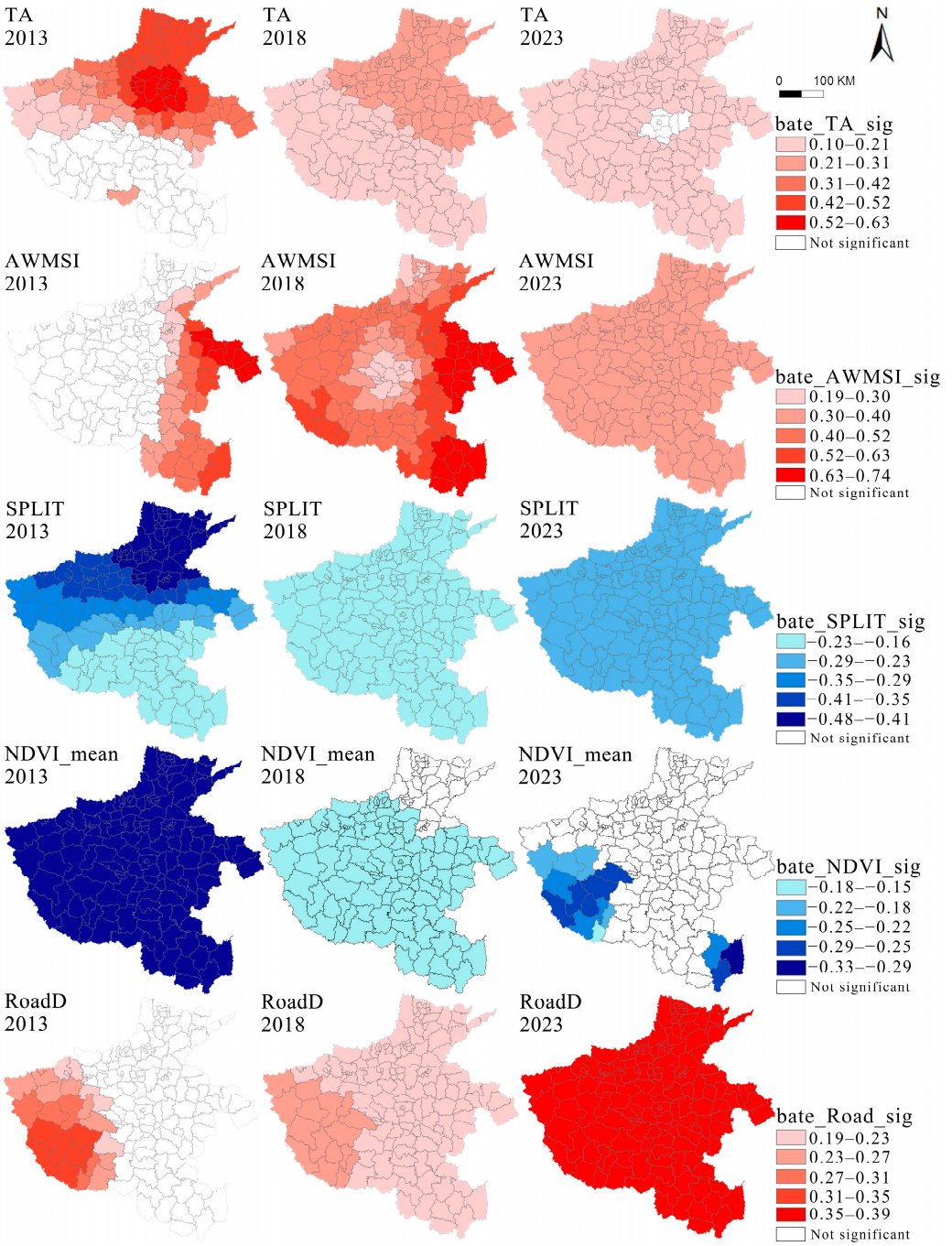


Figure 6. Spatial distribution of significant MGWR coefficients in 2013, 2018, and 2023.

Overall, these MGWR results underscore the importance of accounting for spatial non-stationarity when examining the determinants of county-level CEP. The influence of urban–rural landscape configuration and ecological indicators is highly heterogeneous, and local effects vary across regions and over time. These findings complement the cross-sectional multiple regression analysis and provide empirical evidence for targeted regional policy interventions to improve carbon emission performance.

3.5.3. Comparison of Cross-Sectional Multiple Regression and MGWR for CEP Analysis

To verify the robustness of the relationships between urban–rural landscape patterns and county-level CEP, both the cross-sectional multiple regression model and the MGWR model were employed. The directions of influence for all explanatory variables remain

largely consistent across the three study years under both models, indicating that the regression results are relatively robust (see Table 7).

Table 7. Regression coefficient comparison.

Variable	Cross-Sectional Multiple Regression			MGWR		
	2013	**2018**	**2023**	**2013**	**2018**	**2023**
R^2	0.69	0.78	0.79	0.76	0.82	0.83
β_1	0.280	0.202	0.165	0.411	0.223	0.120
β_2	0.225	0.435	0.333	0.438	0.468	0.326
β_3	−0.262	−0.216	−0.245	−0.336	−0.175	−0.239
β_4	−0.274	−0.154	−0.139	−0.305	−0.162	−0.240
β_5	0.114	0.204	0.341	0.267	0.212	0.382
β_6	0.256	0.132	0.096	0.257	0.115	0.076

Dependent variable: ln(CEP). β_1 = ln(TA), β_2 = AWMSI, β_3 = SPLIT, β_4 = NDVI_mean, β_5 = ln(RoadD), and β_6 = NTL.

Specifically, TA and AWMSI exhibit positive effects in both models, suggesting that larger construction land scale and more complex patch shapes are generally associated with higher CEP. In contrast, SPLIT shows a negative effect, indicating that high spatial fragmentation tends to reduce carbon emission performance. RoadD generally has a positive effect, reflecting the contribution of improved transportation infrastructure to regional carbon efficiency. NDVI_mean shows a negative relationship with CEP, capturing the interactions between ecological background conditions and regional development stages. NTL has a positive effect in some years but is not consistently significant.

Regarding explanatory power, the MGWR model demonstrates higher goodness of fit than the cross-sectional multiple regression model across all three years, reflecting spatial heterogeneity of variable effects. Compared with the global regression model, MGWR is better able to capture regional differences and reveal the spatially varying relationships between landscape patterns and CEP, highlighting the importance of considering local effects in policy design and spatial planning.

4. Discussion

The analysis of county-level CEP in Henan Province reveals that urban–rural spatial patterns exert significant but spatially heterogeneous influences on carbon efficiency, as evidenced by both cross-sectional multiple regression and MGWR models. The cross-sectional multiple regression results indicate that total construction TA and AWMSI generally exert positive effects on CEP, while SPLIT consistently inhibits carbon efficiency [11,19–21]. NDVI_mean generally shows a negative association with CEP, reflecting the complex interactions between vegetation coverage, industrial activity, and urban development, whereas road density contributes positively to CEP. NTL, as a proxy for industrial activity and energy consumption, shows a positive effect in 2013 and 2018 but becomes insignificant by 2023.

MGWR results further highlight the spatial heterogeneity of these effects. The positive influence of TA is most pronounced in northeastern and central-eastern counties, particularly in 2013, suggesting that counties with relatively intensive urban development benefit most from construction land expansion. This effect diminishes and becomes more uniform across the province by 2018 and 2023, indicating that the influence of construction scale is context dependent, moderated by local development intensity and regional policy implementation. AWMSI exhibits stronger positive effects in central and eastern counties, where irregular and complex urban forms coincide with dense development, while western and southwestern counties show lower or non-significant effects. SPLIT maintains a

negative effect across counties, though its spatial impact weakens over time, reflecting the gradual effectiveness of urban planning policies and land-use regulations that promote compact development [13,15].

NDVI_mean demonstrates negative local effects in 2013, particularly in southern and western counties, indicating that areas with higher vegetation coverage often exhibit lower CEP, likely due to lower industrial intensity or less urbanized activity. By 2018 and 2023, these negative effects moderate in central counties, as industrial and urban development patterns evolve, suggesting a dynamic interplay between ecological background and carbon efficiency [30,42]. RoadD positively affects CEP, with more pronounced impacts in southern and central-eastern counties in 2023. Better-connected road networks facilitate efficient logistics, centralized energy use, and more optimal distribution of industrial activity, thereby enhancing county-level carbon efficiency.

Overall, the comparison between cross-sectional multiple regression and MGWR results demonstrates that while global models capture general trends, MGWR uncovers local variation, revealing that the magnitude and direction of landscape effects on CEP differ across regions and over time.

Based on these results, several policy recommendations can be proposed to enhance CEP through targeted urban planning:

(1) Formulate targeted landscape strategies: Counties with intensive urban development should promote compact and complex urban land configurations to enhance carbon efficiency. Clear planning boundaries and coordination of land use can help reduce inefficient expansion and fragmentation.
(2) Integrate landscape considerations into master planning: Local governments should optimize land-use planning and functional zoning to support sustainable urban development. Mixed-use structures and better access to public facilities can improve energy utilization and promote low-carbon transitions.
(3) Promote rational land arrangements and ecological preservation: Consolidation of scattered parcels, protection of ecological land, and strategic industrial clustering can reduce CO_2 emissions and improve carbon efficiency.
(4) Encourage regional collaboration for low-carbon governance: Establishing joint management systems, zoning guidance, and CO_2 trading mechanisms can enhance inter-county coordination and facilitate emission reductions.

While these strategies can improve CEP and support long-term environmental sustainability, several challenges in policy implementation are noted. Heterogeneity in economic development, industrial structure, and urban scale across counties complicates the formulation of personalized urban strategies. Rapid urbanization can result in increased resource consumption and transportation infrastructure pressures, while technological capacities may be insufficient to fully mitigate carbon emissions. Coordinating multiple stakeholders, including government agencies, enterprises, and the public, further complicates the effective execution of these policies. In addition, the findings of this study also provide practical implications for spatial planning and regional governance. Counties characterized by fragmented construction land and dispersed spatial configurations may benefit from compact development strategies, coordinated infrastructure allocation, and optimized land-use arrangements to improve carbon efficiency. Future studies may further incorporate planning-oriented indicators, such as population density, impervious surface dynamics, and detailed urban development intensity, to enhance the practical applicability of county-level low-carbon development research.

Finally, some limitations of this study should be acknowledged. First, the temporal coverage of the data is limited to 2013, 2018, and 2023, which constrains the analysis of long-term trends. Second, some production inputs and energy consumption indicators are

approximated, which may introduce measurement errors. Third, labor input and industrial heterogeneity are not fully captured, limiting the comprehensiveness of the efficiency measurement. Future research could extend the temporal range, incorporate additional multidimensional input–output indicators, and explore simulation-based scenarios to further understand the dynamic effects of urban–rural spatial development on CEP.

5. Conclusions

This study examined county-level CEP in Henan Province and investigated the impacts of urban–rural landscape patterns using SBM-based efficiency measurement, cross-sectional multiple regression, and MGWR for 2013, 2018, and 2023 [3,4,38]. The analysis highlights substantial spatial heterogeneity in CEP across counties. High-performance counties are concentrated in northeastern and central-eastern regions, while low-performance counties persist in the southwest and south. Over time, CEP improved in central counties, reflecting industrial upgrading, enhanced energy efficiency, and targeted local policies.

Regarding landscape patterns, TA and AWMSI exhibit positive effects on CEP, suggesting that larger and more complex urban land configurations promote carbon efficiency. In contrast, SPLIT consistently shows a negative effect, indicating that fragmented land-use patterns inhibit CEP. NDVI_mean demonstrates negative local effects, particularly in southern and western counties, which may be associated with areas exhibiting lower levels of industrial activity or less intensive urban development. RoadD generally contributes positively, especially in well-connected central-eastern and southern counties, while NTL show positive effects in earlier years but diminish by 2023, suggesting that shifts in industrial activity and energy consumption alter their relationship with CEP over time [11,19–21].

MGWR results further reveal the importance of spatial heterogeneity. The local effects of landscape and ecological variables vary across regions and years, demonstrating that uniform policies may not fully capture county-level CEP dynamics. Compared with cross-sectional multiple regression models, MGWR effectively identifies these spatially varying relationships, providing nuanced insights into the mechanisms through which urban–rural spatial configurations influence carbon efficiency [31].

These findings carry important implications for urban planning and low-carbon policy. Compact and complex urban landscapes, integrated landscape strategies in master planning, preservation of ecological land, and enhanced transportation infrastructure can improve county-level carbon efficiency. Tailored interventions are essential to account for heterogeneity in industrial structure, urbanization pace, and local conditions. The study provides empirical evidence to guide differentiated regional policies and sustainable urban development strategies.

In conclusion, county-level CEP is strongly shaped by urban–rural spatial patterns, and the combined application of SBM and MGWR offers a robust framework to assess both global and local effects, informing targeted interventions for low-carbon development.

Author Contributions: Conceptualization, S.Z. (Shaowei Zhang) and C.Z.; methodology, X.G. and S.Z. (Shaowei Zhang); software, X.G.; validation, S.Z. (Shaowei Zhang), C.Z., S.Z. (Shennian Zhang) and C.L.; formal analysis, X.G.; investigation, X.G.; resources, S.Z. (Shaowei Zhang) and C.Z.; data curation, X.G., S.Z. (Shennian Zhang) and C.L.; writing—original draft preparation, X.G.; writing—review and editing, S.Z. (Shaowei Zhang) and C.Z.; visualization, X.G.; supervision, S.Z. (Shaowei Zhang) and C.Z.; project administration, S.Z. (Shaowei Zhang); funding acquisition, S.Z. (Shaowei Zhang) All authors have read and agreed to the published version of the manuscript.

Funding: This research was supported by the Henan Provincial Soft Science Research Program (Grant No. 252400410525).

Data Availability Statement: Data supporting the findings of this study are available from the corresponding author upon reasonable request.

Conflicts of Interest: The authors declare no conflict of interest.

Abbreviations

The following abbreviations are used in this manuscript:

CEP	Carbon Emission Performance
SBM	Slack-Based Measure
Super-SBM	Super-efficiency Slack-Based Measure
DEA	Data Envelopment Analysis
OLS	Ordinary Least Squares
MGWR	Multiscale Geographically Weighted Regression
TA	Total Area (Construction Land Scale)
AWMSI	Area-Weighted Mean Shape Index
SPLIT	Splitting Index
NDVI	Normalized Difference Vegetation Index
NDVI_mean	Mean Normalized Difference Vegetation Index
RoadD	Road Network Density
DMU	Decision-Making Unit

References

1. Nordhaus, W. Climate Change: The Ultimate Challenge for Economics. *Am. Econ. Rev.* **2019**, *109*, 1991–2014. [CrossRef]
2. Charnes, A.; Cooper, W.; Rhodes, E. Measuring the Efficiency of Decision-Making Units. *Eur. J. Oper. Res.* **1978**, *2*, 429–444. [CrossRef]
3. Dyckhoff, H.; Allen, K. Measuring Ecological Efficiency with Data Envelopment Analysis (DEA). *Eur. J. Oper. Res.* **2001**, *132*, 312–325. [CrossRef]
4. Tone, K. A slacks-based measure of efficiency in data envelopment analysis. *Eur. J. Oper. Res.* **2001**, *130*, 498–509. [CrossRef]
5. Tian, J.; Song, X.; Zhang, J. Spatial-Temporal Pattern and Driving Factors of Carbon Efficiency in China: Evidence from Panel Data of Urban Governance. *Energies* **2022**, *15*, 2536. [CrossRef]
6. Wang, G.; Deng, X.; Wang, J.; Zhang, F.; Liang, S. Carbon Emission Efficiency in China: A Spatial Panel Data Analysis. *China Econ. Rev.* **2019**, *56*, 101313. [CrossRef]
7. He, Q.; Wei, F.; Deng, X.; Kong, F.; Li, C.; Yan, Z.; Qi, Y. Spatiotemporal Pattern of Carbon Productivity and Carbon Offset Potential in Chinese Counties. *Sci. Total Environ.* **2022**, *846*, 157153. [CrossRef]
8. Ma, L.; Cheng, T.; Xiang, L.; Wang, C.; Wei, L.; Wang, J.; Dang, C.; Fu, W.; Wu, H. Chinese Cities Show Disparity Trends in Carbon Efficiency: A Hybrid Approach Combining Explainable Machine Learning and Econometrics. *Sustain. Cities Soc.* **2025**, *127*, 106455. [CrossRef]
9. Li, Y.; Chen, Y. Development of an SBM-ML Model for the Measurement of Green Total Factor Productivity: The Case of Pearl River Delta Urban Agglomeration. *Renew. Sustain. Energy Rev.* **2021**, *145*, 111131. [CrossRef]
10. Jin, Y.; Xu, Y. Carbon Reduction of Urban Form Strategies: Regional Heterogeneity in Yangtze River Delta, China. *Land Use Policy* **2024**, *141*, 107154. [CrossRef]
11. Li, S.; Zhou, C.; Wang, S.; Hu, J. Dose Urban Landscape Pattern Affect CO_2 Emission Efficiency? Empirical Evidence from Megacities in China. *J. Clean. Prod.* **2018**, *203*, 164–178. [CrossRef]
12. Shi, K.; Xu, T.; Li, Y.; Chen, Z.; Gong, W.; Wu, J.; Yu, B. Effects of Urban Forms on CO_2 Emissions in China from a Multi-Perspective Analysis. *J. Environ. Manag.* **2020**, *262*, 110300. [CrossRef]
13. Feng, X.; Wang, S.; Li, Y.; Yang, J.; Lei, K.; Yuan, W. Spatial Heterogeneity and Driving Mechanisms of Carbon Emissions in Urban Expansion Areas: A Research Framework Coupled with Patterns and Functions. *Land Use Policy* **2024**, *143*, 107209. [CrossRef]
14. Wu, H.; Yang, Y.; Li, W. Spatial Optimization of Land Use and Carbon Storage Prediction in Urban Agglomerations under Climate Change: Different Scenarios and Multiscale Perspectives of CMIP6. *Sustain. Cities Soc.* **2024**, *116*, 105920. [CrossRef]
15. Kang, T.; Wang, H.; He, Z.; Liu, Z.; Ren, Y.; Zhao, P. The Effects of Urban Land Use on Energy-Related CO_2 Emissions in China. *Sci. Total Environ.* **2023**, *870*, 161873. [CrossRef]
16. Wan, B.; Sun, Y.; Shen, N.; Sheng, Q.; Yang, T. The Impact of Urban Spatial Configuration on Carbon Emissions: Towards Spatial Planning for Low-Carbon Development. *Sustain. Futur.* **2025**, *9*, 100559. [CrossRef]

17. Zhang, S.; Xue, Y.; Jin, S.; Chen, Z.; Cheng, S.; Wang, W. Does Urban Polycentric Structure Improve Carbon Emission Efficiency? A Spatial Panel Data Analysis of 279 Cities in China from 2012 to 2020. *ISPRS Int. J. Geo-Inf.* **2024**, *13*, 462. [CrossRef]
18. Lyu, S.; Huang, Y.; Sun, T. Urban Sprawl, Public Transportation Efficiency and Carbon Emissions. *J. Clean. Prod.* **2025**, *489*, 144652. [CrossRef]
19. Qu, Y.; Zhan, L.; Zhang, Q.; Si, H.; Jiang, G. Towards Sustainability: The Impact of the Multidimensional Morphological Evolution of Urban Land on Carbon Emissions. *J. Clean. Prod.* **2023**, *424*, 138888. [CrossRef]
20. Tang, Z.; Wang, Y.; Fu, M.; Xue, J. The Role of Land Use Landscape Patterns in the Carbon Emission Reduction: Empirical Evidence from China. *Ecol. Indic.* **2023**, *156*, 111176. [CrossRef]
21. Han, X.; Fu, M.; Wang, J.; Li, S. Optimizing Territorial Spatial Structures Within the Framework of Carbon Neutrality: A Case Study of Wuan. *Land* **2024**, *13*, 1147. [CrossRef]
22. Jin, Y.; Xu, Y. The Divergent Effects of Polycentric Urban Form on Urban Carbon Emissions: Spatial Balance and Spatial Dispersion in Chinese Cities. *Urban Clim.* **2024**, *55*, 101862. [CrossRef]
23. Wang, C.; Zhang, Y.; Chen, J.; Li, D.; Zhu, M.; Gan, Z. The Impact of Urban Polycentricity on Carbon Emissions: A Case Study of the Yangtze River Delta Region in China. *J. Clean. Prod.* **2024**, *442*, 141127. [CrossRef]
24. Li, R.; Han, X.; Wang, Q. Do Technical Differences Lead to a Widening Gap in China's Regional Carbon Emissions Efficiency? Evidence from a Combination of LMDI and PDA Approach. *Renew. Sustain. Energy Rev.* **2023**, *182*, 113361. [CrossRef]
25. Liu, C.; Hu, S.; Wu, S.; Song, J.; Li, H. County-Level Land Use Carbon Emissions in China: Spatiotemporal Patterns and Impact Factors. *Sustain. Cities Soc.* **2024**, *105*, 105304. [CrossRef]
26. Xie, Z.; Wu, R.; Wang, S. How Technological Progress Affects the Carbon Emission Efficiency? Evidence from National Panel Quantile Regression. *J. Clean. Prod.* **2021**, *307*, 127133. [CrossRef]
27. Liu, C.; Wang, X.; Li, H. County-Level Land Use Carbon Budget in the Yangtze River Economic Belt, China: Spatiotemporal Differentiation and Coordination Zoning. *Land* **2024**, *13*, 215. [CrossRef]
28. Bhatta, B.; Saraswati, S.; Bandyopadhyay, D. Urban sprawl measurement from remote sensing data. *Appl. Geogr.* **2010**, *30*, 731–740. [CrossRef]
29. Bibri, S.E.; Krogstie, J.; Karrholm, M. Compact City Planning and Development: Emerging Practices and Strategies for Achieving the Goals of Sustainability. *Dev. Built Environ.* **2020**, *4*, 100021. [CrossRef]
30. Creutzig, F.; Baiocchi, G.; Bierkandt, R.; Pichler, P.-P.; Seto, K.C. Global Typology of Urban Energy Use and Potentials for an Urbanization Mitigation Wedge. *Proc. Natl. Acad. Sci. USA* **2015**, *112*, 6283–6288. [CrossRef]
31. Dong, L. Spatio-temporal Evolution and Prediction of Carbon Balance in the Yellow River Basin and Zoning for Low-Carbon Economic Development. *Sci. Rep.* **2024**, *14*, 14385. [CrossRef]
32. He, J.; Hu, S. Ecological Efficiency and Its Determining Factors in an Urban Agglomeration in China: The Chengdu-Chongqing Urban Agglomeration. *Urban Clim.* **2022**, *41*, 101071. [CrossRef]
33. Wang, Y.; Luo, X.; Chen, W.; Zhao, M.; Wang, B. Exploring the Spatial Effect of Urbanization on Multi-Sectoral CO_2 Emissions in China. *Atmos. Pollut. Res.* **2019**, *10*, 1610–1620. [CrossRef]
34. Wang, Y.; Niu, Y.; Li, M.; Yu, Q.; Chen, W. Spatial Structure and Carbon Emission of Urban Agglomerations: Spatiotemporal Characteristics and Driving Forces. *Sustain. Cities Soc.* **2022**, *78*, 103600. [CrossRef]
35. Gim, T.-H.T. Analyzing the City-Level Effects of Land Use on Travel Time and CO_2 Emissions: A Global Mediation Study of Travel Time. *Int. J. Sustain. Transp.* **2022**, *16*, 496–513. [CrossRef]
36. Guan, D.; Peters, G.P.; Weber, C.L.; Hubacek, K. Journey to World Top Emitter: An Analysis of the Driving Forces of China's Recent CO_2 Emissions Surge. *Geophys. Res. Lett.* **2009**, *36*, L04709. [CrossRef]
37. Liu, Z.; Guan, D.; Wei, W.; Davis, S.J.; Ciais, P.; Bai, J.; Peng, S.; Zhang, Q.; Hubacek, K.; Marland, G.; et al. Reduced Carbon Emission Estimates from Fossil Fuel Combustion and Cement Production in China. *Nature* **2015**, *524*, 335–338. [CrossRef]
38. Chen, Y.; Xu, J.-T. An Assessment of Energy Efficiency Based on Environmental Constraints and Its Influencing Factors in China. *Environ. Sci. Pollut. Res. Int.* **2019**, *26*, 16887–16900. [CrossRef]
39. Fan, S.-C.; Liu, H.-Y.; Wang, X.-P.; He, W.-T. Spatio-Temporal Correlation Between Green Space Landscape Pattern and Carbon Emission in Three Major Coastal Urban Agglomerations. *Environ. Sci.* **2025**, *46*, 3509–3523. [CrossRef]
40. Shi, C.; Guo, N.; Gao, X.; Wu, F. How Carbon Emission Reduction is Going to Affect Urban Resilience. *J. Clean. Prod.* **2022**, *372*, 133737. [CrossRef]

41. Sha, W.; Chen, Y.; Wu, J.; Wang, Z. Will Polycentric Cities Cause More CO_2 Emissions? A Case Study of 232 Chinese Cities. *J. Environ. Sci.* **2020**, *96*, 33–43. [CrossRef]
42. Zhang, X.; Meng, Q.; Xu, J.; Li, K. Urbanization Impacts on Anthropogenic Carbon Dioxide Emissions and the Roles of Urban Morphologies: Insights from Urban Socioeconomic Clusters and Local Climate Zones in Shanghai, China. *Sustain. Cities Soc.* **2025**, *129*, 106494. [CrossRef]

Disclaimer/Publisher's Note: The statements, opinions and data contained in all publications are solely those of the individual author(s) and contributor(s) and not of MDPI and/or the editor(s). MDPI and/or the editor(s) disclaim responsibility for any injury to people or property resulting from any ideas, methods, instructions or products referred to in the content.